Inorg. Chem. **2007**, *46*, 3971–3983

Vanadium(V) Tartrato Complexes: Speciation in the $H_3O^+(OH^-)/H_2VO_4^-/$(2*R*,3*R*)-Tartrate System and X-ray Crystal Structures of $Na_4[V_4O_8(rac\text{-tart})_2]\cdot 12H_2O$ and $(NEt_4)_4[V_4O_8((R,R)\text{-tart})_2]\cdot 6H_2O$ (tart = $C_4H_2O_6^{4-}$)

Peter Schwendt,*,† Alan S. Tracey,‡ Jozef Tatiersky,† Jana Gáliková,† and Zdirad Žák§

Department of Inorganic Chemistry, Faculty of Natural Sciences, Comenius University, Mlynská dolina, Bratislava 84215, Slovak Republic, Department of Chemistry, Simon Fraser University, Burnaby, British Columbia V5A 1S6, Canada, and Department of Inorganic Chemistry, Faculty of Natural Sciences, Masaryk University, Kotlářská 2, Brno 61137, Czech Republic

Received November 22, 2006

A study of the aqueous $H_3O^+(OH^-)/H_2VO_4^-/$(2*R*,3*R*)-tartrate system has been performed at 273 K in a 1.0 mol/L $Na^+(Cl^-)$ ionic medium using ^{51}V NMR spectroscopy. In this relatively complicated system, more than 12 different species were observed. Ligand concentration, vanadate concentration, and pH variation studies were carried out, particularly for the range of pH 5.8–8.0 and for pH 2.4. Chemical shifts, vanadium–ligand stoichiometry, and also composition and formation constants for some, but not all, species are given. Despite some reduction of vanadium(V) to vanadium(IV) in an acidic medium at pH ≈2.4, the stoichiometries of the principal species in solution at this pH were determined. Electrospray ionization mass spectra for some solutions were obtained and were in accordance with the conclusions drawn from the speciation studies. A series of crystalline vanadium(V) tartrato complexes $M_4[V_4O_8(tart)_2]\cdot aq$ were also prepared and characterized. X-ray diffraction studies of $Na_4[V_4O_8(rac\text{-tart})_2]\cdot 12H_2O$ (**1**) and $(NEt_4)_4[V_4O_8((R,R)\text{-tart})_2]\cdot 6H_2O$ (**2**) revealed unique tetranuclear $[V_4O_8(tart)_2]^{4-}$ ions for which the $\{V_4O_4\}$ rings have boat conformations.

Introduction

The anions of α-hydroxycarboxylic acids take part in many basic biochemical processes and thus represent an important group of biogenic ligands. All crystallographically characterized α-hydroxycarboxylato complexes of vanadium(V) possess a dinuclear structure[1] with a $\{V_2O_2\}$ ring, where the bridging O atoms derive from the α-hydroxyl groups of the ligands.

Complexation of vanadium(V) with tartaric acid has been studied since 1939. Solution studies utilizing UV−vis spectroscopy,[2] conductometry,[2] cryoscopy,[2] IR spectroscopy,[3] and ^1H, ^{13}C, and ^{51}V NMR spectroscopy,[4] polarography,[5] and cyclic voltammetry[5] have been carried out. From the very often controversial interpretation of experimental results, the existence of complexes with $n(V)/n(tart^{n-})$ ratios 4, 2, 1, and 0.5 has been proposed. Caldeira et al.[4] using NMR spectroscopy, irrespective of the vanadate/D-tartaric acid molar ratio, observed only one complex [$\delta(^{51}V) = -522$ ppm] throughout the range of pH 3.0−7.5. A tetranuclear

* To whom correspodence should be addressed. E-mail: schwendt@fns.uniba.sk.
† Comenius University.
‡ Simon Fraser University.
§ Masaryk University.

(1) (a) Zhou, Z. H.; Wang, J. Z.; Wan, H. L.; Tsai, K. R. *Chem. Res. Chin. Univ.* **1994**, *10*, 102−106. (b) Smatanová, I.; Marek, J.; Švančárek, P.; Schwendt, P. *Acta Crystallogr.* **1998**, *C54*, 1249−1251. (c) Hambley, T. W.; Judd, R. J.; Lay, P. A. *Inorg. Chem.* **1992**, *31*, 343−345. (d) Wright, D. W.; Humiston, P. A.; Orme-Johnson, W. H.; Davis, W. M. *Inorg. Chem.* **1995**, *34*, 4194−4197. (e) Zhou, Z. H.; Yan, W. B.; Wan, H. L.; Tsai, K. R.; Wang, J. Z.; Hu, S. Z. *J. Chem. Crystallogr.* **1995**, *25*, 807−811. (f) Zhou, Z. H.; Wan, H. L.; Hu, S. Z.; Tsai, K. R. *Inorg. Chim. Acta* **1995**, *237*, 193−197. (g) Wright, D. W.; Chang, R. T.; Mandal, S. K.; Armstrong, W. H.; Orme-Johnson, W. H. *J. Biol. Inorg. Chem.* **1996**, *1*, 143−151. (h) Švančárek, P.; Schwendt, P.; Tatiersky, J.; Smatanová, I.; Marek, J. *Monatsh. Chem.* **2000**, *131*, 145−154. (i) Djordjevic, C.; Lee, M.; Sinn, E. *Inorg. Chem.* **1989**, *28*, 719−723. (j) Djordjevic, C.; Lee-Renslo, M.; Sinn, E. *Inorg. Chim. Acta* **1995**, *233*, 97−102. (k) Smatanová, I.; Švančárek, P.; Marek, J.; Schwendt, P. *Acta Crystallogr.* **2000**, *C56*, 154−155. (l) Schwendt, P.; Švančárek, P.; Smatanová, I.; Marek, J. *J. Inorg. Biochem.* **2000**, *80*, 59−64. (m) Schwendt, P.; Ahmed, M.; Marek, J. *Inorg. Chim. Acta* **2005**, *358*, 3572−3580 and references cited therein. (n) Kaliva, M.; Raptopoulou, C. P.; Terzis, A.; Salifoglou, A. *Inorg. Chem.* **2004**, *43*, 2895−2905 and references cited therein. (o) Hati, S.; Batchelor, R. J.; Einstein, F. W. B.; Tracey, A. S. *Inorg. Chem.* **2001**, *40*, 6258−6265. (p) Biagioli, M.; Strinna-Erre, L.; Micera, G.; Panzanelli, A.; Zema, M. *Inorg. Chim. Acta* **2000**, *310*, 1−9.

10.1021/ic062223h CCC: $37.00
Published on Web 04/10/2007

structure with a planar $\{V_4O_4\}$ ring has been suggested for this complex.[3−6] More recently, on the basis of ligand concentration studies using ^{51}V NMR spectroscopy, two complexes were identified, with the major product being specified as a 1:1 V/tart complex.[5] It is evident that there is little agreement between the various studies.

Two types of solid complexes have been obtained by reactions of vanadates with tartaric acid or tartrates: (a) relatively stable red complexes $M_2O{\cdot}V_2O_5{\cdot}C_4H_4O_5{\cdot}$aq (M = Na, K, Rb, Cs, $^1/_2$Mg, $^1/_2$Ca) and (b) unstable yellow compounds formulated as $3M_2O{\cdot}2V_2O_5{\cdot}2C_4H_4O_5{\cdot}$aq (M = K, Rb, Cs, $^1/_2$Ca).[2] These results have been confirmed by Sivák,[3,7] who has proposed a dinuclear structure for yellow complexes and a planar tetranuclear structure for red ones.

In this study, ^{51}V NMR spectroscopy was used to determine speciation in the aqueous $H_3O^+(OH^-)/H_2VO_4^-$/(2*R*,3*R*)-tartrate system. Electrospray ionization mass spectrometry (ESIMS) was used to substantiate the results of the speciation analysis. Also, we report the syntheses and characterization of a series of vanadium(V) tartrato complexes and the X-ray crystal structures of $Na_4[V_4O_8(rac\text{-tart})_2]{\cdot}12H_2O$ and $(NEt_4)_4[V_4O_8((R,R)\text{-tart})_2]{\cdot}6H_2O$.

Experimental Section

Materials and Syntheses. V_2O_5 was prepared by thermal decomposition (at 773 K) of previously purified NH_4VO_3. KVO_3 was prepared by thermal decomposition (at 393 K) of $KVO_3{\cdot}xH_2O$ obtained by reaction of V_2O_5 with an aqueous solution of KOH at pH 8. For preparation of the solutions for the NMR measurements, $NaVO_3{\cdot}2H_2O$ (p.a., Lachema) and (2*R*,3*R*)-tartaric acid (p.a., Lachema) were used. All other chemicals were of reagent grade and were used as commercially obtained without further purification.

$Na_4[V_4O_8(rac\text{-tart})_2]{\cdot}12H_2O$ (1). $NaVO_3$ (1.22 g, 10.0 mmol) was dissolved in water (7.5 mL). To the cold solution (278 K) was added under continuous stirring an aqueous solution of *rac*-tartaric acid (5 mL of a 1 mol/L solution, 5 mmol). The red solution that was obtained (pH 5.8) was maintained for a further 2 h at 278 K, and then ethanol was added until the first turbidity occurred. Dark-red crystals were isolated after 2 h of standing at 278 K. Anal. Calcd for $C_8H_{28}Na_4O_{32}V_4$ (found): C, 10.3 (10.2); H, 3.0 (2.8); V, 21.9 (22.3). IR bands (2000−400 cm^{-1}): 1645 vs [ν_{as}(COO$^-$)], 1361 s [ν_s(COO$^-$)], 1320 m, 1292 m, 1273 w, 1250 w, 1236 w, 1217 w, 1210 w, 1088 m [ν(C−O$_h$)] (O$_h$ = oxygen atom of the hydroxylic group of the tartrato ligand), 1078 s [ν(C−O$_h$)], 1060 m [ν(C−O$_h$)], 1049 m [ν(C−O$_h$)], 971 vs [ν(V=O$_t$)] (O$_t$ = terminal oxygen atom), 936 sh, 917 w, 850 m, 766 vs [ν_{as}(VOV)], 711 m, 660 m [ν_s(VOV)], 622 sh, 598 sh, 554 s [ν(V−O$_{tart}$)] (O$_{tart}$ = coordinated oxygen atom of the tartrato ligand), 517 w, 489 m, 440 m, 414 m.

$(NEt_4)_4[V_4O_8((R,R)\text{-tart})_2]{\cdot}6H_2O$ (2). V_2O_5 (0.18 g, 1.0 mmol) was dissolved in a NEt_4OH solution (2 mL of a 2.34 mol/L solution, 4.86 mmol), and an aqueous solution of (2*R*,3*R*)-tartaric acid was added (2 mL of a 1 mol/L solution, 2 mmol). The pH of the red solution was 6.3. For initiation of crystallization, acetone was added. After 5 days of standing at 276 K, large red plates were isolated. Anal. Calcd for $C_{40}H_{96}N_4O_{26}V_4$ (found): C, 38.3 (38.9); H, 7.7 (8.3); N, 4.5 (4.7); V, 16.3 (15.7). IR bands (2000−400 cm^{-1}): 1632 vs [ν_{as}(COO$^-$)], 1594 vs, 1352 m [ν_s(COO$^-$)], 1325 m, 1299 m, 1171 s, 1097 s [ν(C−O$_h$)], 1071 m [ν(C−O$_h$)], 1000 s, 957 vs [ν(V=O$_t$)], 930 m, 854 m, 823 m, 797 sh, 777 w, 739 s [ν_{as}(VOV)], 656 m [ν_s(VOV)], 632 w, 600 w, 546 s [ν(V−O$_{tart}$)], 533 sh, 510 sh, 466 m, 434 m, 403 m.

$Na_4[V_4O_8((R,R)\text{-tart})_2]{\cdot}12H_2O$ (3). $NaVO_3$ (1.22 g, 10.0 mmol) was dissolved in water (7.5 mL). To the cold solution (273 K) was added solid (2*R*,3*R*)-tartaric acid (0.75 g, 5.0 mmol). This provided a red solution, which was maintained at 273 K for 2 h, after which cold ethanol (20 mL) was added. After 14 days at 250 K, red needle-shaped crystals were isolated. Anal. Calcd for $C_8H_{28}Na_4O_{32}V_4$ (found): C, 10.3 (10.1); H, 3.0 (2.9); V, 21.9 (21.7). IR bands (2000−400 cm^{-1}): 1640 vs [ν_{as}(COO$^-$)], 1350 s [ν_s(COO$^-$)], 1339 w, 1330 m, 1301 m, 1279 m, 1248 w, 1216 w, 1085 s [ν(C−O$_h$)], 1059 m [ν(C−O$_h$)], 973 vs [ν(V=O$_t$)], 916 w, 851 m, 829 w, 770 vs [ν_{as}(VOV)], 729 sh, 653 s [ν_s(VOV)], 556 s [ν(V−O$_{tart}$)], 491 m, 440 m, 407 m.

$K_4[V_4O_8((R,R)\text{-tart})_2]{\cdot}8H_2O$ (4). KVO_3 (1.38 g, 10.0 mmol) was dissolved in water (7.5 mL). Upon the addition of solid (2*R*,3*R*)-tartaric acid (0.75 g, 5.0 mmol), a red solution was obtained. To this solution (pH 5.3) was added ethanol until a precipitate started to appear. Red needles were isolated after 24 h of standing at 276 K. Anal. Calcd for $C_8H_{20}K_4O_{28}V_4$ (found): C, 10.4 (10.2); H, 2.2 (2.0); V, 22.0 (22.0). IR bands (2000−400 cm^{-1}): 1633 vs [ν_{as}(COO$^-$)], 1349 s [ν_s(COO$^-$)], 1314 w, 1292 w, 1250 w, 1219 w, 1084 s [ν(C−O$_h$)], 1057 m [ν(C−O$_h$)], 967 vs [ν(V=O$_t$)], 917 m, 851 m, 829 m, 760 vs [ν_{as}(VOV)], 652 s [ν_s(VOV)], 553 s [ν-(V−O$_{tart}$)], 438 m, 407 m.

$K_4[V_4O_8(rac\text{-tart})_2]{\cdot}8H_2O$ (5). KVO_3 (0.69 g, 5.0 mmol) was dissolved in water (5 mL), and an aqueous solution of *rac*-tartaric acid (2.5 mL of a 1 mol/L solution, 2.5 mmol) was added. The pH was adjusted to 3.9 using a 5 mol/L KOH solution. Ethanol was added until the first precipitate was formed. Crystallization at 276 K yielded red plate-shaped crystals. Anal. Calcd for $C_8H_{20}K_4O_{28}V_4$ (found): C, 10.4 (10.4); H, 2.2 (2.2); V, 22.0 (22.8). IR bands (2000−400 cm^{-1}): 1663 vs [ν_{as}(COO$^-$)], 1347 s [ν_s(COO$^-$)], 1316 m, 1292 m, 1271 m, 1249 w, 1207 w, 1095 m [ν(C−O$_h$)], 1083 s [ν(C−O$_h$)], 1057 m [ν(C−O$_h$)], 1045 m [ν(C−O$_h$)], 989 sh, 973 vs [ν(V=O$_t$)], 918 w, 850 m, 790 sh, 768 vs [ν_{as}(VOV)], 659 m [ν_s(VOV)], 557 s [ν(V−O$_{tart}$)], 515 w, 483 w, 436 m, 414 sh.

$(NH_4)_4[V_4O_8((R,R)\text{-tart})_2]{\cdot}9H_2O$ (6). To the aqueous solution of NH_4VO_3 (4 mL of 0.5 mol/L solution, 2 mmol) was added an aqueous solution of (2*R*,3*R*)-tartaric acid (1 mL of a 1 mol/L solution, 1 mmol). Crystallization from the red solution (pH 3.9) was initiated by ethanol. Orange-red plates were isolated after 1 day of standing at 276 K. Anal. Calcd for $C_8H_{38}N_4O_{28}V_4$ (found): C, 11.4 (11.6); H, 4.5 (4.5); N, 6.7 (6.5); V, 24.2 (23.9). IR bands (2000−400 cm^{-1}): 1606 vs [ν_{as}(COO$^-$)], 1409 m [δ_d(NH_4^+)], 1349 s [ν_s(COO$^-$)], 1314 w, 1214 w, 1081 m [ν(C−O$_h$)], 1057 m [ν-(C−O$_h$)], 969 vs [ν(V=O$_t$)], 916 m, 848 m, 830 w, 756 vs [ν_{as}-(VOV)], 650 m [ν_s(VOV)], 554 m [ν(V−O$_{tart}$)], 483 m, 436 m, 407 w.

$(NMe_4)_4[V_4O_8((R,R)\text{-tart})_2]{\cdot}3H_2O$ (7). V_2O_5 (0.18 g, 1.0 mmol) was dissolved in a NMe_4OH aqueous solution (2 mL of a 1.1 mol/L solution, 2.2 mmol). Then aqueous solutions of (2*R*,3*R*)-tartaric acid

(2) Jahr, K. F.; Preuss, F.; Rosenhahn, L. *J. Inorg. Nucl. Chem.* **1969**, *31*, 297−302 and references cited therein.
(3) Sivák, M. *Acta Fac. Rerum Nat. Univ. Comenianae, Chim.* **1981**, *XXIX*, 37−45.
(4) Caldeira, M. M.; Ramos, M. L.; Cavaleiro, A. M.; Gil, V. M. S. *J. Mol. Struct.* **1988**, *174*, 461−466.
(5) Khan, A. R.; Crans, D. C.; Pauliukaite, R.; Norkus, E. *J. Braz. Chem. Soc.* **2006**, *17*, 895−904.
(6) Bartůšek, M.; Šustáček, V. *Collect. Czech. Chem. Commun.* **1983**, *48*, 2785−2797.
(7) Sivák, M. *Acta Fac. Rerum Nat. Univ. Comenianae, Chim.* **1981**, *XXIX*, 47−57.

Table 1. Crystallographic Data and Refinement Results for **1** and **2**

complex	**1**	**2**
formula	$C_8H_{28}Na_4O_{32}V_4$	$C_{40}H_{96}N_4O_{26}V_4$
M (g/mol)	932.02	1252.98
space group	$P\bar{1}$ (No. 2)	$P2_1$ (No. 4)
a (Å)	10.627(2)	12.225(2)
b (Å)	11.392(2)	14.029(3)
c (Å)	14.167(3)	18.298(4)
α (deg)	88.76(3)	90
β (deg)	78.53(3)	108.75(3)
γ (deg)	62.85(3)	90
V (Å^3)	1490.9(5)	2971.6(10)
Z	2	2
ρ_{calcd} (g/mL)	2.076	1.400
temperature (K)	120(2)	120(2)
λ (Å)	0.71073	0.71073
μ (mm^{-1})	1.397	0.689
R1 ($I > 2\sigma_I$)[a]	0.0193	0.0499
wR2 ($I > 2\sigma_I$)[b]	0.0530	0.1173

[a] $R1 = \sum||F_o| - |F_c||/\sum|F_o|$. [b] $wR2 = \{\sum w(F_o^2 - F_c^2/\sum wF_o^2\}^{1/2}$.

2 mL of a 1 mol/L solution, 2 mmol) and NMe_4OH (1.8 mL of a 1.1 mol/L solution, 1.98 mmol) were added. To the red solution (pH 6.8) was added acetone to initiate crystallization. Small red needles crystallized from the solution standing at 276 K after 4 days. Anal. Calcd for $C_{24}H_{58}N_4O_{23}V_4$ (found): C, 29.3 (29.8); H, 6.0 (6.3); N, 5.7 (5.7); V, 20.7 (21.4). IR bands (2000−400 cm^{-1}): 1617 vs [ν_{as}(COO$^-$)], 1485 m, 1335 s [ν_s(COO$^-$)], 1302 m, 1094 s [ν(C−O$_h$)], 1067 m [ν(C−O$_h$)], 958 vs [ν(V=O$_t$)], 915 m, 852 m, 825 m, 799 m, 759 vs [ν_{as}(VOV)], 704 w, 658 m [ν_s(VOV)], 603 m, 555 s [ν(V−O$_{tart}$)], 481 m, 434 w.

Physical Measurements. The IR spectra were recorded on a Nicolet Magna 750 Fourier transform IR spectrometer with either Nujol mulls or KBr tablets. Elemental analysis (C, H, and N) was performed on a 1106 CHN analyzer (Carlo Erba, Milano, Italy). Vanadium(V) was determined gravimetrically as V_2O_5 in a platinum crucible at 773 K or volumetrically by titration with $FeSO_4$ (c = 0.1 mol/L) using diphenylamine as the indicator. UV−vis spectra were recorded on a Jasco V-530 UV−vis spectrophotometer at room temperature. ^{51}V NMR spectra were recorded at 278 or 295 K on a Varian Mercury Plus 300 MHz spectrometer operating at 78.94 MHz (^{51}V) and a Varian Unity Inova 600 MHz spectrometer operating at 157.68 MHz (^{51}V) in 5 mm tubes without locking on D_2O. Chemical shifts are in ppm relative to a $VOCl_3$ external reference, also determined at 278 or 295 K. ESIMS spectra were recorded for x, y, and z using a direct probe on a Waters ZMD 2000 mass spectrometer. The mass spectrometer was directly coupled to a MassLynx data system. Solutions for ESIMS were prepared by mixing solutions of (2*R*,3*R*)-tartaric acid, $NaVO_3$, and NaOH [c(H_4tart), 0.01 or 0.06 mol/L; c($NaVO_3$), 0.0018 or 0.01 mol/L; pH, 3.0, 4.1, or 4.6]. The pH was measured with a Precision digital pH meter OP-208/1 (Radelkis, Budapest, Hungary) by use of a combined semimicro pH electrode HC 139 (THETA '90). The log β values for the proton−ligand complexes were estimated by standard potentiometric procedures.

Solutions for the NMR Measurements. Stock aqueous solutions of 0.15 mol/L $NaVO_3$·$2H_2O$, 1.00 mol/L (2*R*,3*R*)-tartaric acid, 0.20 mol/L HEPES buffer, and 4.00 mol/L NaCl were used for mixing of solutions for measurement. The pH of the solution was adjusted by adding a NaOH solution (1 or 0.1 mol/L) or a HCl solution (only for solutions with pH 2.4; c(HCl), 2 or 0.1 mol/L). All final solutions were prepared with c(Na^+) = 1.0 mol/L. The solutions for the NMR measurements were prepared by combining appropriate amounts from the various stock solutions in the following order: (2*R*,3*R*)-tartaric acid, NaCl, HEPES, (H_2O), (NaOH), $NaVO_3$, (NaCl), (HCl), H_2O. Careful adherence to procedure meant that decavanadate was not formed, even at low tartrate concentrations at pH 6.5. Solutions were allowed to stand approximately 3 h for equilibration before the measurement. Depending on pH, some increase of the pH (up to 0.2 pH units) with time occurred as a result of the reduction of vanadium(V) to vanadium(IV). Reduction was faster in acidic solutions. By monitoring the changes of the intensity of the band characteristic for the vanadium(IV) complex at 762 nm, we estimate that at pH 2.4 up to 10% of the total vanadium was reduced when the measurement was finished. This had a negative impact on the speciation procedure, particularly at low pH. The problem was, however, mitigated to an extent by cooling the samples to 278 K. To compare our data with those in the literature,[8] some spectra were measured for solutions at different conditions: 295 K; a 0.6 mol/L Na^+(Cl^-) ionic medium.

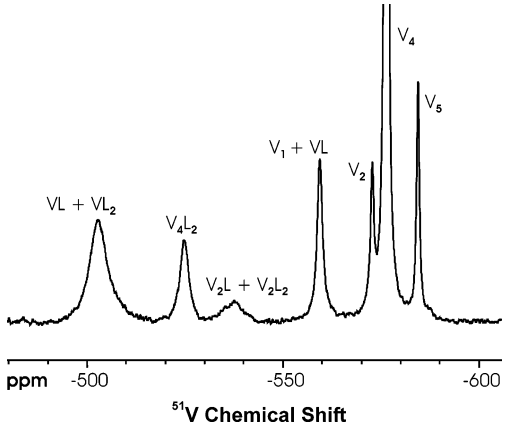

Figure 1. ^{51}V NMR spectrum obtained at 157.68 MHz showing vanadate, several of its oligomers, and a number of tartrate complexes. Conditions of the experiment: vanadate, 3.0 mmol/L; (2*R*,3*R*)-tartaric acid, 30.0 mmol/L; pH, 6.5; HEPES buffer, 20 mmol/L; temperature, 278 K; a 1.0 mol/L Na^+(Cl^-) ionic medium.

Crystal Structure Determination. The intensity data were collected on a KUMA KM-4 κ-axis diffractometer using a graphite-monochromatized Mo Kα radiation equipped with an Oxford Cryosystem LT device and corrected for absorption effects using a ψ scan. The ω-scan technique with different κ and φ offsets for covering an independent part of reflections in the 2−25° θ range was used. The cell parameters were refined from all strong reflections. The data reductions were carried out using the *CrysAlis RED* (Oxford Diffraction, Abingdon, U.K.) program. The structures were determined by *SHELXS-97*[9] and refined by *SHELXL-97*,[10] and the data for publication were prepared by *SHELXL* and *PARST*[11] and the figures by *Diamond*.[12] Crystal data and structure determination summaries for **1** and **2** are listed in Table 1. Selected bond lengths and angles for the two compounds are listed in Table 2.

Results and Discussion

Speciation in the H_3O^+(OH^-)/$H_2VO_4^-$/(2*R*,3*R*)-Tartrate System. Vanadium, tartrate, and hydrogen ion concentration studies were undertaken in order to identify the products formed in solution and to elucidate their stoichiometries. Preliminary studies at pH 6.5 showed the presence of three products with ^{51}V NMR chemical shifts of −503, −524, and

(8) Pettersson, L.; Hedmann, B.; Andersson, I.; Ingri, N. *Chem. Scr.* **1983**, *22*, 254−264.
(9) Sheldrick, G. M. *Acta Crystallogr.* **1990**, *A46*, 467−473.
(10) Sheldrick, G. M.; Schneider, T. R. *Methods Enzymol.* **1997**, *277*, 319−343.
(11) Nardelli, M. *Comput. Chem.* **1983**, *7*, 95−97.
(12) *DIAMOND*, version 3.1.d; CRYSTAL IMPACT: Bonn, Germany.

Table 2. Selected Bond Lengths (Å) and Angles (deg) for **1** and for **2**

	complex			complex	
	1	**2**		**1**	**2**
V1−O13	1.5970(14)	1.618(4)	O14−V2−O20	102.32(7)	103.51(18)
V1−O17	1.7727(13)	1.759(4)	O14−V2−O3	100.80(6)	100.95(19)
V1−O18	1.8201(12)	1.828(4)	O20−V2−O3	100.53(6)	98.52(17)
V1−O4	1.9270(13)	1.963(4)	O14−V2−O19	103.18(6)	104.01(19)
V1−O6	2.0389(13)	2.070(4)	O20−V2−O19	90.31(6)	91.65(17)
V2−O14	1.5916(14)	1.618(4)	O3−V2−O19	150.86(6)	149.97(15)
V2−O20	1.8304(13)	1.854(4)	O14−V2−O1	100.74(7)	99.32(17)
V2−O3	1.8573(13)	1.869(4)	O20−V2−O1	156.71(5)	157.14(17)
V2−O19	1.8826(12)	1.884(4)	O3−V2−O1	78.17(5)	78.12(16)
V2−O1	2.0375(13)	2.059(4)	O19−V2−O1	81.29(6)	81.58(16)
V3−O15	1.5923(12)	1.602(4)	O15−V3−O20	102.35(6)	103.22(19)
V3−O20	1.8317(12)	1.838(4)	O15−V3−O9	100.93(7)	100.99(18)
V3−O9	1.8413(14)	1.882(4)	O20−V3−O9	100.00(6)	99.74(17)
V3−O17	1.8747(15)	1.889(4)	O15−V3−O17	101.38(6)	103.79(18)
V3−O7	2.0269(13)	2.070(4)	O20−V3−O17	90.81(6)	91.75(16)
V4−O16	1.5995(12)	1.617(4)	O9−V3−O17	152.44(6)	149.44(16)
V4−O19	1.7814(13)	1.783(4)	O15−V3−O7	103.56(6)	100.74(17)
V4−O18	1.8104(13)	1.823(4)	O20−V3−O7	153.80(5)	155.91(16)
V4−O10	1.9314(12)	1.962(4)	O9−V3−O7	78.81(6)	77.96(15)
V4−O12	2.0398(16)	2.070(4)	O17−V3−O7	80.40(6)	80.09(16)
O13−V1−O17	106.98(7)	105.39(18)	O16−V4−O19	105.70(6)	107.16(19)
O13−V1−O18	102.01(6)	102.61(18)	O16−V4−O18	102.43(7)	102.18(18)
O17−V1−O18	98.84(6)	98.93(16)	O19−V4−O18	97.64(6)	98.18(17)
O13−V1−O4	108.34(7)	110.64(18)	O16−V4−O10	107.74(6)	108.40(18)
O17−V1−O4	141.68(6)	141.79(16)	O19−V4−O10	144.11(5)	142.20(16)
O18−V1−O4	87.98(5)	85.49(16)	O18−V4−O10	87.64(6)	86.55(15)
O13−V1−O6	94.96(6)	93.21(18)	O16−V4−O12	94.97(6)	93.45(19)
O17−V1−O6	84.77(6)	88.32(16)	O19−V4−O12	86.59(6)	87.53(16)
O18−V1−O6	160.68(5)	160.06(16)	O18−V4−O12	160.16(5)	160.85(15)
O4−V1−O6	77.88(5)	77.53(15)	O10−V4−O12	77.95(6)	77.98(15)

−537 ppm. Figure 1 shows a ^{51}V NMR spectrum obtained from a 600 MHz spectrometer.

Several product signals are observable in this spectrum and, in anticipation of the analysis, are identified in the figure. Also identified are the various oligomeric vanadates that typically are found. It should be noted that, under the conditions of this study, decavanadate is not observed in the NMR spectra. Additionally, line broadening and a change in the chemical shift of close to −0.5 ppm of the V_1 signal indicated the formation of products in rapid equilibration with V_1. Similar behavior has been found for α-hydroxycarboxylic acids and has been assigned to the presence of products deriving from monodentate carboxylate and hydroxylate coordination.[13,14] In the case of lactate, the overall formation constant for these products was 0.55 ± 0.05 M^{-1} at pH 7.35.[14] Because of the statistical factor, this value can be expected to approximately double for the tartrate system.

A major complication in this study was the extreme sensitivity of product formation to the pH of the medium. Going from pH 6.5 to 7.0 was sufficient to eliminate the major product signal at −524 ppm and the minor product signal at −537 ppm from the NMR spectra. This presented one advantage in that the product giving rise to the −503 ppm signal could be studied in isolation. For the analysis, the tetramer was used as the reference compound for two reasons. The principal one is that this compound gives a relatively sharp NMR signal, and therefore its concentration is accurately determined relative to the other components. Also, it has a charge state that is constant at 4−, with it not being protonated under acidic conditions, which makes it a good reference for studies under conditions of different pH.[15−17]

Two products are observed in the NMR spectrum at pH 7.9. The one of initial interest is a minor component in rapid equilibration with the monomer, V_1. As mentioned, this is possibly two components deriving from an independent monodentate reaction at the hydroxyl and carboxylate groups. Because the V/L stoichiometry is identical for the two situations, it is not possible to separate the two formation constants at fixed pH, and only an overall formation constant, K_f, is available. Reaction proceeds according to eq 1, but because $[V_1]$ is not known, V_4 provides a reference for V_1 according to eq 2 so that the two formation constants, K'_{14} and K_f, are provided by eq 3, where cV_1 is the total concentration of V_1 components ($cV_1 = [V_1] + [VL]$) represented by the mixed signal. The equilibrium unligated tartrate concentration, $[L^{2-}]$, is obtained from the conservation equation for total L, so an initial analysis is required in order to determine ligand stoichiometry for the various products. Corrections to [L] are then applied as the analysis proceeds. The two pK_a values of tartaric acid are 2.68 ± 0.02 and 3.55 ± 0.02 under the conditions of the NMR experiments. These values compare well with the literature

(13) Tracey, A. S.; Li, H.; Gresser, M. J. *Inorg. Chem.* **1990**, *29*, 2267−2271.
(14) Tracey, A. S.; Gresser, M. J.; Parkinson, K. M. *Inorg. Chem.* **1987**, *26*, 629−638.
(15) Elvingson, K.; Baro, A. G.; Pettersson, L. *Inorg. Chem.* **1996**, *35*, 3388−3393.
(16) Pettersson, L.; Hedman, B.; Nenner, A. M.; Andersson, I. *Acta Chem. Scand.* **1985**, *A39*, 499−506.
(17) Pettersson, L.; Andersson, I.; Hedman, B. *Chem. Scr.* **1985**, *25*, 309−317.

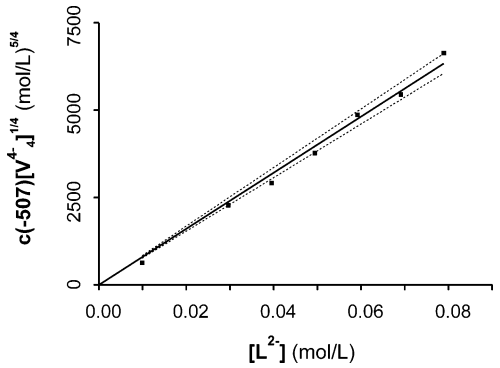

Figure 2. Graphical representation of the formation of the product giving rise to the −507 ppm signal. The solid line gives the least-squares fit to a straight line, while the dotted lines represent the 95% confidence interval. Conditions of the experiments: total vanadate, 6.0 mmol/L; (2*R*,3*R*)-tartaric acid, variable 10−80 mmol/L; pH, 7.95; HEPES buffer, 20 mmol/L; temperature, 278 K; all solutions, a 1.0 mol/L $Na^+(Cl^-)$ ionic medium.

values[18] of 2.69 and 3.73 at $I = 1.0$ mol/L. These low pK_a values mean that it is not necessary to consider any but the doubly minus charge state of the ligand unless the pH is well below 6.

$$V_1 + L \rightleftharpoons VL \qquad [V_1][L]K_f = [VL] \tag{1}$$

$$4V_1 \rightleftharpoons V_4 \qquad [V_1]^4K'_{14} = [V_4] \tag{2}$$

$$cV_1/[V_4]^{1/4} = (1 + [L]K_f)/K'_{14}{}^{1/4} \tag{3}$$

A plot of the left side of eq 3 vs [L] then provides both K'_{14} and K_f. The values obtained were $K'_{14} = (3.6 \pm 0.5) \times 10^9$ M^{-3} and $K_f = 1.1 \pm 0.7$ M^{-1}. The value for K_f is only poorly determined, but it and K'_{14} are in line with expectations from other studies.[13,14] This value of K'_{14} is not a true formation constant in the sense that, at this pH, the signal from V_1 corresponds to V_1 in two ionic states, V_1^- and V_1^{2-}. Knowing K'_{14} allows the constant for formation of the −507 ppm product from V_1 to be ascertained even though V_4 is used as the reference compound. Preliminary studies suggested that the −507 ppm product had VL stoichiometry and thus is formed as described by eq 1, with K_{VL} replacing K_f. On this basis, eq 4 is obtained, where the product is identified by its NMR chemical shift.

$$c(-507) = [L][V_4]^{1/4}K_{VL}/K'_{14}{}^{1/4} \tag{4}$$

Figure 2 gives a graphical representation of the experimental results plotted according to eq 4 when the total vanadate concentration was held constant and the tartrate concentration varied. A similarly good graph was obtained when the ligand was maintained constant and the vanadate concentration varied. K_{VL} had the values 19.7 ± 0.4 M^{-1} and 19.1 ± 0.3 M^{-1} from the tartrate and vanadate concentration studies, respectively. There was no indication that the −507 ppm signal was a composite signal deriving from more than one component.

(18) Kotrlý, S.; Šůcha, L. *Handbook of Chemical Equilibria in Analytical Chemistry;* Ellis Horwood Ltd.: Chichester, U.K., 1985.

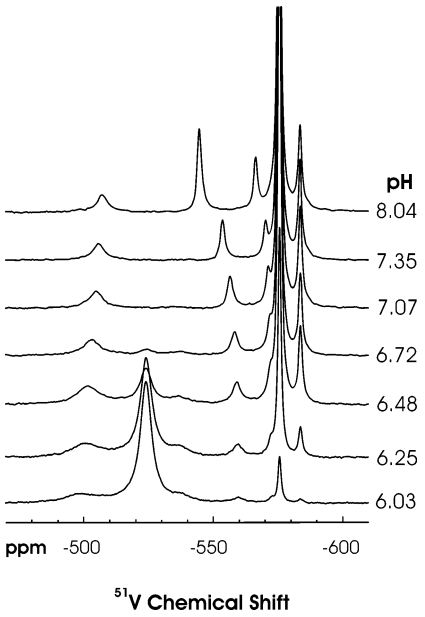

Figure 3. ^{51}V NMR spectra showing the influence of the pH throughout the range of pH 6.0−8.0 on equilibria in the aqueous vanadate/(2*R*,3*R*)-tartrate system. Conditions of the experiments: total vanadate, 6.0 mmol/L; (2*R*,3*R*)-tartaric acid, 30.0 mmol/L; pH, as indicated; HEPES buffer, 20 mmol/L; temperature, 278 K; all solutions, a 1.0 mol/L $Na^+(Cl^-)$ ionic medium.

Figure 3 shows the influence of the pH on the ^{51}V NMR spectra for the range of pH 6.0−8.0. It is evident that, as the pH becomes lower, the NMR spectra become considerably more complicated. This is in accordance with a more complicated speciation at the lower pH. Variation of the vanadate and ligand concentrations at pH 6.5 clearly showed that the various products have different stoichiometries.

The pH variation studies showed that the −507 ppm signal shifted to lower field upon acidification from pH 8.0 and occurred at −503 ppm at pH 6.5. In accordance with this, the vanadate concentration studies showed that the −503 ppm signal corresponded to monovanadate species. However, the ligand concentration study showed that the −503 ppm signal had components from both VL (eq 1) and VL_2 (eq 5) products, unlike what was observed at higher pH, where only VL was observed. Therefore, the concentration corresponding to the −503 ppm signal, $c(-503)$, is given by eq 6, which can be rewritten in terms of the V_4 concentration and formation constants as eq 7, where K_{14} represents the formation of V_4^{4-} from $4V_1^-$.

$$V_1 + 2L \rightleftharpoons VL_2 \qquad [V_1][L]^2K_{VL_2} = [VL_2] \tag{5}$$

$$c(-503) = [VL] + [VL_2] \tag{6}$$

$$\frac{c(-503)}{[V_4]^{1/4}[L]} = K_{VL}/K_{14}{}^{1/4} + K_{VL_2}[L]/K_{14}{}^{1/4} \tag{7}$$

Formation of the −503 ppm products is sensitive to the pH. The observations suggested that there is formation of three complexes, VL^{3-}, HVL^{2-}, and HVL_2^{4-}, as described by eqs 8−12.

$$V_1^- + L^{2-} \rightleftharpoons VL^{3-} \qquad [V_1^-][L^{2-}]K_{VL} = [VL^{3-}] \quad (8)$$

$$VL^{3-} + H^+ \rightleftharpoons HVL^{2-} \qquad [VL^{3-}][H^+]K_{HVL} = [HVL^{2-}] \quad (9)$$

$$HVL^{2-} + L^{2-} \rightleftharpoons HVL_2^{4-} \qquad [HVL^{2-}][L^{2-}]K_{HVL_2} = [HVL_2^{4-}] \quad (10)$$

$$c(-503) = [VL^{3-}] + [HVL^{2-}] + [HVL_2^{4-}] \quad (11)$$

$$\frac{c(-503)}{[V_4^{4-}]^{1/4}[L^{2-}]} = (K_{VL} + K_{VL}K_{HVL}[H^+] + K_{VL}K_{HVL}K_{HVL_2}[H^+][L^{2-}])/K_{14}^{1/4} \quad (12)$$

A plot of the term on the left side of eq 12 vs $[H^+]$ gave a graph with a small amount of curvature. Extrapolation of the curve to the *Y* axis gave an intercept of 0.0708 ± 0.0015, which equals $K_{VL}/K_{14}^{1/4}$ or $K_{VL} = 42.0 \pm 1.1$ M^{-1}. This is in good agreement with the pH 7.9 study where the proportion of V_1^- in total V_1 ($V_1^- + V_1^{2-}$) is close to $^1/_2$ that at pH 6.5, thus reducing the formation constant of VL from V_1^- by a factor of about 2. An additional correction is needed if significant protonation of VL^{3-} occurs at pH 6.5.

That there is a HVL_2^{4-} component can be seen from a ligand concentration study. This is demonstrated most readily by rearranging eq 12 into a form linear in $[L^{2-}]$. The graph gives both a slope and an intercept when the appropriate data obtained from tartrate concentration studies are plotted (Figure 1s in the Supporting Information). The *Y* intercept would be zero if no HVL^{2-} were formed, while the slope would be zero if no HVL_2^{4-} were formed.

There was no evidence that HVL_2^{4-} loses a proton with an increase in the pH. The formation of HVL_2^{4-} becomes progressively unfavored as the pH is increased with respect to VL^{3-}, and it consequently is not formed to a great extent at elevated pH, in accordance with a VL_2 product not being observed in the pH 7.9 study. The value determined for the pK_a of HVL^{2-} from the *Y* intercept of the graph was 6.04. The formation constants for these and the other products are summarized in Table 3. The formation constants are written in the log β_{pqr} notation defined by $H_pV_qL_r$, with $H_2VO_4^-$ being the reference, V_1, from which the stoichiometry is defined and for which *q* is 1 and *p* and *r* are 0.

The −537 ppm signal is quite broad, and this, coupled with the comparatively low signal intensity, adds uncertainty to the analysis. The vanadium concentration study at fixed tartrate concentration was consistent with this product having V_2 stoichiometry. No evidence was obtained for a V_3 component, which might have been expected because products of V_3 stoichiometry are frequently formed with α-hydroxycarboxylic acids and give rise to chemical shifts near this frequency.[19,20] Analysis of the ligand concentration study proved somewhat more problematic and suggested that

Table 3. Formation Constants of (2*R*,3*R*)-Tartrate (L) Complexes of Vanadium[a]

formula/notation[b]	*p*, *q*, *r*	log $\beta_{pqr}(3\sigma)$	δ_V (ppm)[c]
HVO_4^{2-}	−1, 1, 0	−7.87(3)	−534
$H_2VO_4^-$	0, 1, 0		−560
$HV_2O_7^{3-}$	−1, 2, 0	−5.03(4)	−572
$H_2V_2O_7^{2-}$	0, 2, 0	3.00(6)	−561
$V_4O_{12}^{4-}$	0, 4, 0	10.92(7)	−576
$V_5O_{15}^{5-}$	0, 5, 0	13.61(9)	−584
VL^{3-}	0, 1, 1	1.62(3)	−507
HVL^{2-}	1, 1, 1	7.68(4)	−503
HVL_2^{4-}	1, 1, 2	9.36(4)	−503
HV_2L^{3-}	1, 2, 1	10.23(19)	−537
$H_2V_2L_2^{4-}$	2, 2, 2	18.62(10)	−537
$H_3V_4L_2^{5-}$	3, 4, 2	32.55(9)	−524
$H_4V_4L_2^{4-}$	4, 4, 2	39.03(9)	−524

[a] Formation constants are for the following conditions: total vanadate, 6 mmol/L; (2*R*,3*R*)-tartaric acid, 30 mmol/L; pH, variable 5.8−8.0; HEPES buffer, 20 mmol/L; temperature, 278 K; all solutions, a 1.0 mol/L $Na^+(Cl^-)$ ionic medium. [b] Oxygen stoichiometry is not specified for the tartrato complexes because full stoichiometry may be uncertain. [c] Except for VL^{3-}, which is for a pH 7.9 solution, the chemical shifts observed for the tartrate complexes are for pH 6.5. Because of signal overlap, or possibly rapid exchange, the signals near −503 ppm and those near −537 ppm are average values measured for a broad signal.

the −537 ppm signal corresponded to products of V_2L and V_2L_2 stoichiometry. In this event, formation of the −537 ppm products proceeds according to eqs 13 and 14, and their formation from V_4 can be written as in eq 15. In accordance with this assignment, the agreement between the assumed stoichiometry and the experimental results, when plotted according to eq 15, is good (Figure 2s in the Supporting Information).

$$2V_1 + L \rightleftharpoons V_2L \qquad [V_1]^2[L]K_{V_2L} = [V_2L] \quad (13)$$

$$2V_1 + 2L \rightleftharpoons V_2L_2 \qquad [V_1]^2[L]^2K_{V_2L_2} = [V_2L_2] \quad (14)$$

$$\frac{c(-537)}{2[V_4]^{1/2}[L]} = (K_{V_2L} + [L]K_{V_2L_2})/K_{14}^{1/2} \quad (15)$$

Analysis of the pH variation data showed that only one proton per ligand was taken up during formation of each of the two −537 ppm products (eqs 16 and 17). Equation 18 gives the conservation equation for the products giving rise to the −537 ppm signal. This can be combined with eqs 16 and 17, rewritten as eq 19, and the experimental results plotted graphically (Figure 3s in the Supporting Information).

$$H^+ + 2V_1^- + L^{2-} \rightleftharpoons HV_2L^{3-} \qquad [H^+][V_1^-]^2[L]K_{HV_2L} = [HV_2L^{3-}] \quad (16)$$

$$2H^+ + 2V_1^- + 2L^{2-} \rightleftharpoons H_2V_2L_2^{4-} \qquad [H^+]^2[V_1^-]^2[L]^2K_{H_2V_2L_2} = [H_2V_2L_2^{4-}] \quad (17)$$

$$c(-537)/2 = [HV_2L^{3-}] + [H_2V_2L_2^{4-}] \quad (18)$$

The intercept of the graph is small but cannot be said to be 0. From the formation constants for pH 6.5 with 6.0 mmol/L total vanadate and 30 mmol/L (2*R*,3*R*)-tartaric acid, it can be calculated that there is a little over twice as much

(19) Gorzsas, A.; Andersson, I.; Pettersson, L. *J. Chem. Soc., Dalton Trans.* **2003**, 2503−2511.
(20) Tracey, A. S. *Coord. Chem. Rev.* **2003**, *237*, 113−121.

$$\frac{c(-537)}{2[V_4^{4-}]^{1/2}[L^{2-}][H^+]} = (K_{HV_2L} + K_{H_2V_2L_2}[L^{2-}][H^+])/K_{14}^{1/2} \quad (19)$$

of the bisligand than of the monoligand complex in solution. These studies only provide stoichiometry and cannot determine whether V_2L_2 is similar to V_2L with a second ligand attached or whether they are completely different products.

There were no indications from any studies that the −524 ppm signal was a composite signal deriving from more than a single product. The vanadate and tartrate concentration studies showed that the −524 ppm product had four vanadium centers and was complexed by two tartrate ligands. Its formation, therefore, is described by eqs 20 and 21. A graphical representation of the data, when plotted according to eq 21, gave an excellent straight line (Figure 4s in the Supporting Information).

$$4V_1 + 2L \rightleftharpoons V_4L_2 \qquad [V_1]^4[L]^2K_{V_4L_2} = [V_4L_2] \quad (20)$$

$$c(-524)/4 = [V_4][L]^2K_{V_4L_2}/K_{14} \quad (21)$$

The pH study of this product was particularly interesting because, although it showed that four protons were taken up during formation of the −524 ppm product, one of the protons could be released; that is to say, $H_3V_4L_2^{5-}$ can form. This is described by eqs 22−24.

$$4H^+ + 4V_1^- + 2L^{2-} \rightleftharpoons H_4V_4L_2^{4-} \qquad [H^+]^4[V_1^-]^4[L^{2-}]^2K_{H_4V_4L_2} = [H_4V_4L_2^{4-}] \quad (22)$$

$$3H^+ + 4V_1^- + 2L^{2-} \rightleftharpoons H_3V_4L_2^{5-} \qquad [H^+]^3[V_1^-]^4[L^{2-}]^2K_{H_3V_4L_2} = [H_3V_4L_2^{5-}] \quad (23)$$

$$\frac{c(-524)}{4[V_4^{4-}][L^{2-}]^2[H^+]^3} = (K_{H_3V_4L_2} + K_{H_4V_4L_2}[H^+])/K_{14} \quad (24)$$

A graph of the quantities of eq 24 is shown in Figure 4. If the intercept of this graph were 0, no $H_3V_4L_2^{5-}$ would be found in solution. If $H_4V_4L_2^{4-}$ and $H_3V_4L_2^{5-}$ differ only by the presence of the single proton, then the pK_a of $H_4V_4L_2^{4-}$ is 6.48. There are no protons available in $H_4V_4L_2^{4-}$ unless it has complexed water. This result therefore suggests that the coordination about vanadium in an aqueous solution is not pentacoordinate as observed in the crystalline material but rather more highly coordinated, perhaps hexacoordinate (see the discussion of the crystal structure).

A summary of the formation constants measured is given in Table 3. These values were used to obtain a species distribution diagram (Figure 5) for the range of pH 6−8 and calculated for 6 mmol/L total vanadate and 30 mmol/L (2*R*,3*R*)-tartaric acid.

An effort was made to identify species occurring at pH 2.4. A titration from pH 6.01 to 2.55 (Figure 6) suggested that there was no change in the identity of the product giving rise to the −524 ppm signal because this signal remained

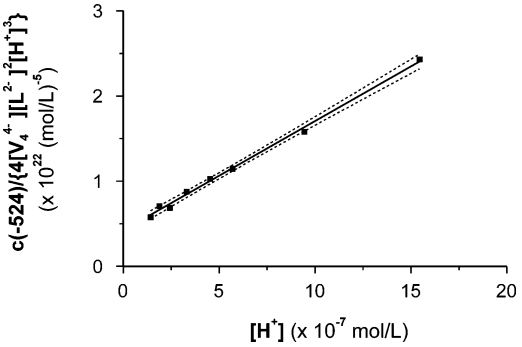

Figure 4. pH dependence of the formation of the tetranuclear products giving rise to the −524 ppm signal. The intercept corresponds to the formation of $V_4L_2H^{3-}$ and the slope to $V_4L_2H_2^{4-}$. The solid line gives the least-squares fit to a straight line, while the dotted lines represent the 95% confidence interval. Conditions of the experiments: total vanadate, 6.0 mmol/L; (2*R*,3*R*)-tartaric acid, 30 mmol/L; pH, variable 5.81−8.04; HEPES buffer, 20 mmol/L; temperature, 278 K; all solutions, a 1.0 mol/L $Na^+(Cl^-)$ ionic medium.

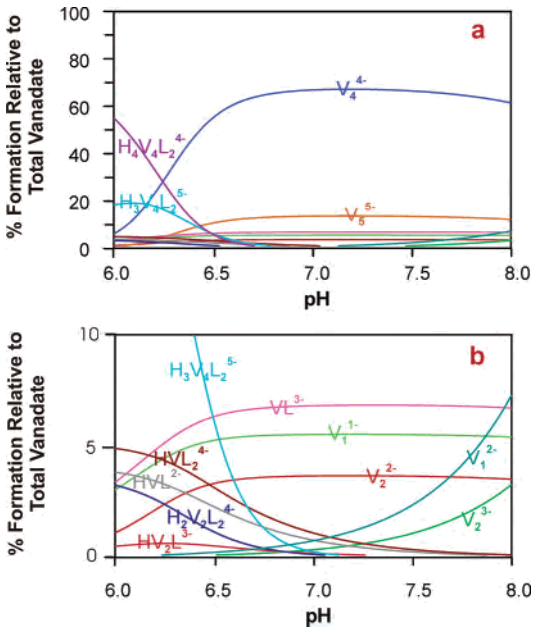

Figure 5. Species distribution diagram calculated for the pH range 6−8. For the calculations, the concentrations were as follows: total vanadate, 6.0 mmol/L; (2*R*,3*R*)-tartaric acid, 30 mmol/L. The formation constants are found in Table 3 and determined for a 1.0 mol/L $Na^+(Cl^-)$ ionic medium.

fixed at −524 ppm and there was no change in the line shape with a change in the pH. However, several additional NMR signals were observed at lower pH.

As demonstrated by Figure 7, the relative intensities of these signals are highly dependent on the amount of tartaric acid (H_3tart^- + H_4tart at pH 2.4) in solution. The principle one of the new signals occurred at −550 ppm. Other signals occurred at −461, −511, −532, and −539 ppm. Under the low pH conditions, there was on the order of 10% reduction of vanadium(V) to vanadium(IV) when the spectra were measured.

Despite this, it was possible to draw some conclusions about species stoichiometry. Over the range of tartaric acid concentrations of 10−60 mmol/L, the V-atom concentration corresponding to the −524 ppm signal decreased from 1.93 mmol/L at 10 mmol/L tartaric acid to 0.14 mmol/L at 60 mmol/L tartaric acid while the V-atom concentration cor-

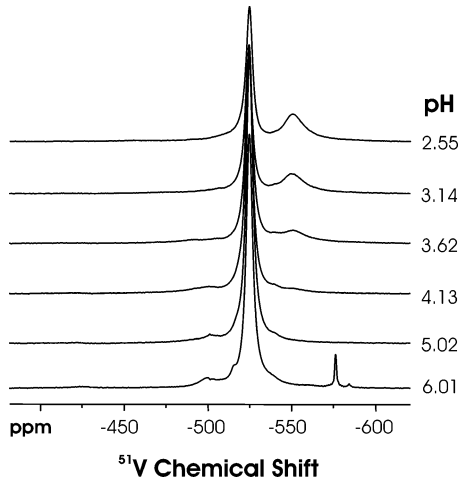

Figure 6. ^{51}V NMR spectra showing the influence of the pH throughout the range of pH 2.55−6.01 on equilibria in the aqueous vanadate/(2*R*,3*R*)-tartrate system. Conditions of the experiments: total vanadate, 30 mmol/L; (2*R*,3*R*)-tartaric acid, 60 mmol/L; pH, as indicated; temperature, 278 K; all solutions, a 1.0 mol/L $Na^+(Cl^-)$ ionic medium.

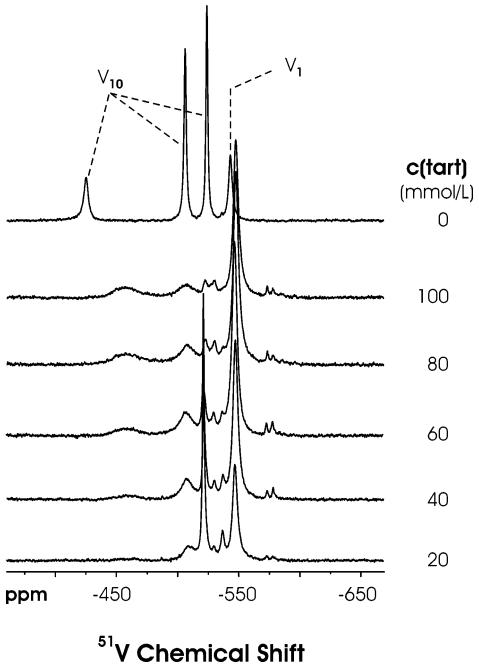

Figure 7. ^{51}V NMR spectra showing the influence of the (2*R*,3*R*)-tartaric acid concentration on equilibria in the aqueous acidic vanadate/(2*R*,3*R*)-tartrate system for (2*R*,3*R*)-tartaric acid concentrations varying throughout the range of 0−100 mmol/L. Conditions of the experiments: total vanadate, 3.0 mmol/L; (2*R*,3*R*)-tartaric acid, as indicated; pH, 2.4; temperature, 295 K; all solutions, a 0.6 mol/L $Na^+(Cl^-)$ ionic medium.

responding to the −550 ppm signals increased from 0.63 to 1.77 mmol/L. On the other hand, the −524 ppm signal increased in intensity much more rapidly than did the −550 ppm signal when the tartaric acid concentration was fixed and the total vanadate concentration was increased. In fact, the behavior was consistent with formation of V_2L_2 from V_4L_2 as described by eq 25, where it is assumed that the −524 ppm signal corresponds to V_4L_2, in accordance with the pH 6.5 studies and the pH titration (Figure 6). The experimental data, when plotted graphically according to eq 25, gave a good linear correlation (Figure 5s in the Supporting Information).

$$V_4L_2 + 2L \rightleftharpoons 2V_2L_2 \qquad [V_4L_2]\,[L]^2\,K = [V_2L_2]^2 \quad (25)$$

If the product is V_2L_2, then, as suggested by a −13 ppm change in the chemical shift from that observed at pH 6.5 for a V_2L_2 product, there is a difference in coordination, perhaps the V center having octahedral rather than pentacoordinate geometry. Possibly there is bridging between V atoms by the tartrate ligands in addition to the normal oxo bridging, or alternatively there may simply be a change in the hydration state. A different coordination is expected because this product was not observable in the NMR spectra until the pH was below 4. Vanadate itself goes from tetrahedral to octahedral coordination under acidic conditions with incorporation of water into the coordination sphere. In the vanadate case, the change in coordination is accompanied by a change in the protonation state. Unfortunately, the charge state of the −550 ppm product is not known.

There is an additional product that appears to have V_2L_2 stoichiometry that gives an NMR signal at −511 ppm. This compound is about a factor of 4 less favored than the −550 ppm product, but its formation with a change in the tartrate concentration follows closely that of the −550 ppm product.

Some information was also obtained about the stoichiometry of the −539 ppm product. Under conditions where the −524 ppm product dropped in concentration by a factor of about 14, the concentration of the −539 ppm product followed lockstep with that of the −524 ppm product. This is demonstrated in Figure 8. The linear correlation suggests that the −524 and −539 ppm products both have the same V/L stoichiometry, i.e., V_4L_2. Because protonation/deprotonation will generally be fast on the NMR time scale unless accompanied by a coordination change, it seems likely that these two tetravanadate complexes differ in their structure.

There is another product that is observed when there is a large excess of ligand in solution (see Figure 7). This product gives rise to a very broad signal at −461 ppm, and its concentration increases rapidly with an increase in the free ligand concentration, being about 0.13 mmol/L at 40 mmol/L tartrate and about 0.45 mmol/L at 60 mmol/L tartrate, both measurements for 3.0 mmol/L total vanadate. For comparison purposes, the concentration of the −550 ppm product (V_2L_2) changes from 1.70 to 1.77 mmol/L while that of the −524 ppm product (V_4L_2) changes from 0.50 to 0.14 mmol/L, for the same two ligand concentrations, respectively. Evidently, the −461 ppm product has a comparatively high L/V stoichiometry, perhaps VL_2.

There is an additional minor product signal that occurs at −530 ppm. This signal was only poorly characterized, but it increases in intensity with an increase in the tartaric acid concentration in a fashion that suggests it has more than a 1:1 V/L stoichiometry. Two other very low intensity signals occurred at −575 and −580 ppm. Their intensities did not vary much over the range of tartaric acid concentrations above 20 mmol/L, where they accounted for about 2% of the total vanadium in the solution. However, it is to be noted that these signals did not occur when no ligand was present and were very weak at 10 mmol/L tartaric acid. They were not more fully characterized.

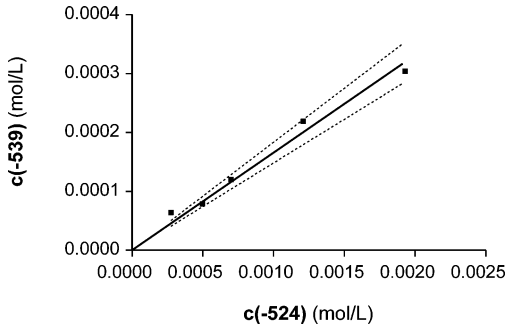

Figure 8. Concentration of the −539 ppm shown as a function of the −524 ppm product as (2*R*,3*R*)-tartaric acid is varied from 10 to 60 mmol/L. The solid line represents a linear least-squares fit to the data and the broken lines the 95% confidence interval. Conditions of the experiments: total vanadate, 3.0 mmol/L; (2*R*,3*R*)-tartaric acid, variable 10−60 mmol/L; pH, 2.40; temperature, 295 K; all solutions, a 0.6 mol/L $Na^+(Cl^-)$ ionic medium.

Table 4. Strongest Signals in the ESIMS Spectrum of the $NaVO_3$−(2*R*,3*R*)-H_4tart−NaOH−H_2O−CH_3OH Solution in Negative Mode[a]

m/z found	*m/z* calcd	relative intensity (%)	assignment	designation in Table 3 and in the text
74.13	74.04	6	H_2tart^{2-}	
116.82	116.95	10	$H_2VO_4^-$	V_1
148.89	149.08	100	H_3tart^-	
156.05	155.97	23	$[V_4O_8(tart)_2]^{4-}$	$H_4V_4L_2^{4-}$
165.06	164.98	92	$[V_4O_8(tart)_2(H_2O)_2]^{4-}$	
208.15	208.29	51	$[V_4O_8(tart)(Htart)_2]^{3-}$	
230.86	231.01	28	$[V_2O_4(H_2tart)_2]^{2-}$	V_2L_2
313.04	312.94	16	$[V_4O_8(Htart)_2]^{2-}$	

[a] $c(NaVO_3) = c(H_4tart) = 10$ mmol/L, pH 3.0, solution:methanol = 9:1 by volume (after measurement of the pH).

The results of the speciation studies are generally confirmed by ESIMS in negative mode. The strongest signals obtained from acidic solutions (pH 3.0) (Table 4) can be assigned to species derived from the $[V_4O_8(tart)_2]^{4-}$ ($H_4V_4L_2^{4-}$) ion, to the $[V_2O_4(H_2tart)_2]^{2-}$ (V_2L_2) ion, and to tartrate anions. The ^{51}V NMR spectrum of the same solution but without methanol exhibited signals at −524 ppm ($H_4V_4L_2^{4-}$, 77%), −550 ppm (V_2L_2, 17%), and −537 ($H_2V_2L_2^{4-}$ + HV_2L^{3-}, 6%).

It should be mentioned that vanadium(IV) also forms dinuclear tartrate complexes $M_4[(VO)_2(tart)_2]\cdot nH_2O$,[21] where the fully deprotonated ligand bridges two V centers. The speciation study of the vanadium(IV) tartrate aqueous system suggested that there are various dinuclear complexes and also minor mononuclear species.[22]

We suppose that the structure of the $H_4V_4L_2^{4-}$ species corresponds to the solid-state structure of the $[V_4O_8(tart)_2]^{4-}$ ion (vide infra). The ^{51}V NMR spectra of saturated, very concentrated aqueous solutions of both **1** and **3** exhibited only one signal at −522 ppm, and the spectra did not change for at least 1 h. This structure offers the possibility of eventual breaking of the V−O_c (O_c = oxygen atom of the carboxylate group) bonds and protonation of the carboxylic groups during the ESIMS process. The most abundant complex ion in the ESIMS spectrum was $[V_4O_8(tart)_2(H_2O)_2]^{4-}$. It was found by the X-ray structure analysis that there is enough space for accommodation of a bridging water molecule in each of the two cavities of the $[V_4O_8(tart)_2]^{4-}$ ion. The existence of bridging water molecules is not rare in structures of α-hydroxycarboxylatovanadium(V) complexes (see, e.g., ref 23) and offers some explanation for the otherwise incomprehensible deprotonation of $H_4V_4L_2^{4-}$ and formation of the $H_3V_4L_2^{5-}$ species.

Chart 1. Characteristic Structure of α-Hydroxycarboxylatovanadates (One of a Number of Stereoisomers)

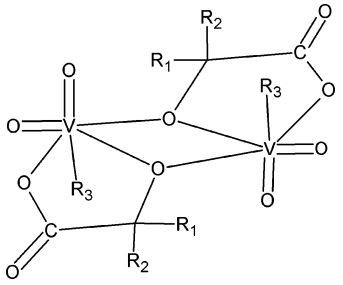

There are some solid tartrato complexes of vanadium(V) that were not fully characterized. Yellow complexes of supposed[7] composition $M^I_3[HV_2O_5(tart)]$ could correspond to the −537 ppm (HV_2L^{3-}) solution species, while the V_2L_2 species (δ_V = −550 ppm) might correspond to the $[V_2O_4(H_2tart)_2]^{2-}$ ion with a dinuclear structure and a $\{V_2O_2\}$ central ring (Chart 1). This type of structure is characteristic for most of the α-hydroxycarboxylatovanadates.

Synthesis and Characterization of Solid Complexes. In spite of there being a number of species present in aqueous solutions, we obtained only complexes of the $M_4[V_4O_8(tart)_2]\cdot$aq type in the form of crystals suitable for X-ray structure determination.

The complexes $Na_4[V_4O_8((R,R)\text{-tart})_2]\cdot 12H_2O$ (**3**), $Na_4[V_4O_8(rac\text{-tart})_2]\cdot 12H_2O$ (**1**), and $K_4[V_4O_8((R,R)\text{-tart})_2]\cdot 8H_2O$ (**4**) were prepared by modified literature methods,[2,24] but we obtained compounds with different numbers of water molecules in comparison with the published data. The complexes $M_4[V_4O_8((R,R)\text{-tart})_2]\cdot nH_2O$ [M = NEt_4 (**2**), NH_4 (**6**), NMe_4 (**7**)] and $K_4[V_4O_8(rac\text{-tart})_2]\cdot 8H_2O$ (**5**) are new. Solid complexes are generally photosensitive: exposure under daylight conditions causes a gradual reduction of vanadium(V), and a color change from red to brown is observed. The most stable of the complexes is $(NEt_4)_4[V_4O_8(R,R\text{-tart})_2]\cdot 6H_2O$ (**2**), which can be stored without decomposition in a refrigerator for weeks and, surprisingly, also aqueous and acetonitrile solutions of this complex preserve their color for several weeks at 276 K and even for several days at room temperature.

(21) (a) Forrest, J. G.; Prout, C. K. *J. Chem. Soc. A* **1967**, 1312−1317. (b) Tapscott, R. E.; Belford, R. L.; Paul, I. C. *Inorg. Chem.* **1968**, *7*, 356−364.
(22) Kiss, T.; Buglyó, P.; Sanna, D.; Micera, G.; Decock, P.; Dewaele, D. *Inorg. Chim. Acta* **1995**, *239*, 145−153.
(23) Schwendt, P.; Švančárek, P.; Kuchta, L.; Marek, J. *Polyhedron* **1998**, *17*, 2161−2166.
(24) Sivák, M. *Acta Fac. Rerum Nat. Univ. Comenianae, Chim.* **1980**, *XXVIII*, 69−75.

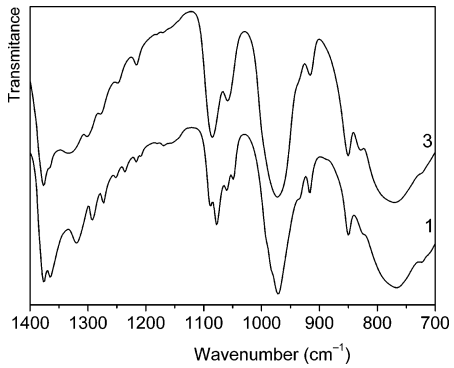

Figure 9. IR spectra of **3** and **1** (1400−700 cm^{-1}).

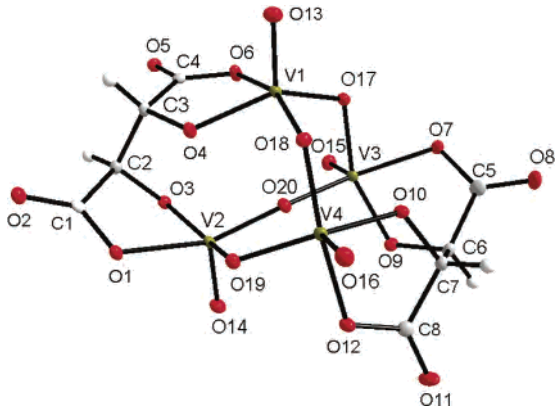

Figure 10. Structure of the $[V_4O_8(R,R\text{-tart})_2]^{4-}$ anion in **1**.

The IR spectra of prepared complexes exhibit characteristic bands corresponding to $\nu_{as}(COO^-)$, $\nu_s(COO^-)$, $\nu(C-O_h)$, $\nu(V=O_t)$, $\nu_{as}(V-O-V)$, $\nu_s(V-O-V)$, and $\nu(V-O_{tart})$ vibrations (see the Experimental Section). The IR spectra of complexes with *rac*- and (2*R*,3*R*)-tartaric acid are very similar. The corresponding bands are only slightly shifted, thus indicating a similar structure of both complexes (Figure 9).

Nevertheless, some splitting of the IR bands was observed in the spectra of *rac*-tartaric acid complexes when compared to the spectra of complexes with (2*R*,3*R*)-tartaric acid, probably a result of correlation effects in the unit cell. This splitting is characteristic, especially in the region of stretching vibrations of $C-O_h$ groups (1100−1000 cm^{-1}; Figure 9). The complexes prepared with *rac*- or (2*R*,3*R*)-tartaric acid can be reliably distinguished by means of these bands.

Crystal Structures. The crystal structure of **1** consists of Na^+ cations, tetranuclear $[V_4O_8(rac\text{-tart})_2]^{4-}$ anions, and water molecules held together by electrostatic forces and hydrogen bonds. The triclinic unit cell contains two tetranuclear anions with different enantiomers of tartaric acid, $[V_4O_8((R,R)\text{-tart})_2]^{4-}$ and $[V_4O_8((S,S)\text{-tart})_2]^{4-}$; the complex **1** represents a typical example of a racemic compound: $Na_8[V_4O_8((R,R)\text{-tart})_2][V_4O_8((S,S)\text{-tart})_2]\cdot 24H_2O$.

The tetranuclear anion (Figure 10) consists of a $\{V_4O_8\}$ group and two $tart^{4-}$ ligands. The $\{V_4O_8\}$ group is composed of four $V=O_t$ groups that are bridged by four bridging O_b atoms. In contrast to what is observed for most tetranuclear vanadium complexes,[25−27] the four V atoms are not coplanar. The central $\{V_4O_4\}$ ring possesses an approximate boat conformation. Each V atom is pentacoordinate. The geometry of the coordination polyhedra can be described in terms of square pyramids distorted toward trigonal bipyramids. The τ value ($\tau = 0$ for ideal square pyramid; $\tau = 1$ for ideal trigonal bipyramid[28]) is 0.32 for V1, 0.098 for V2, 0.023 for V3, and 0.27 for V4. This arrangement is prevalent for pentacoordinated V atoms.[29]

Tetragonal pseudoplanes of the opposite pyramids around V1 and V2 are nearly parallel (the angle between corresponding planes ≈ 6.5°), and they are nearly perpendicular to pseudoplanes of the neighboring pyramids around V3 and V4 (the angles between corresponding planes are ≈ 76°). The situation is analogous for the pyramids around V3 and V4. Because the same enantiomeric form of the two tartrate ligands is coordinated in one $[V_4O_8(tart)_2]^{4-}$ ion, the square pyramids are mutually shifted in a way that enables weak interactions between V and O atoms from the opposite pyramids (V1−O20, V2−O4, V3−O10, and V4−O20; Figure 10). V atoms thus achieve nearly octahedral coordination geometry. Because these interactions are weak, the V atoms deviate considerably from the tetragonal pseudoplanes (between 0.387 and 0.426 Å).

The $\{V_4O_8\}$ group and eight O donor atoms of ligands form a $\{V_4O_{16}\}$ core, which can be considered as composed of four $\{VO_5\}$ tetragonal pyramids. Each of the $\{VO_5\}$ pyramids contains one O_t atom, two O_b atoms, and two O atoms of the ligand (O_h and O_c). The bridging O_b atoms connect each of the $\{VO_5\}$ pyramids with the two neighboring $\{VO_5\}$ pyramids. The bond lengths in the $\{V_4O_{16}\}$ core are within the expected ranges: 1.5946−1.6150 Å for $V=O_t$ bonds; 1.7747−1.8792 Å for $V-O_b$ bonds; 1.8408−

(25) Crans, D. C.; Jiang, F. L.; Chen, J.; Anderson, O. P.; Miller, M. M. *Inorg. Chem.* **1997**, *36*, 1038−1047.
(26) Jiang, F. L.; Anderson, O. P. Miller, S. M.; Chen, J.; Mahroof-Tahir, M.; Crans, D. C. *Inorg. Chem.* **1998**, *37*, 5439−5451.
(27) Tsagkalidis, W.; Rodewald, D.; Rehder, D. *Inorg. Chem.* **1995**, *34*, 1943−1945.
(28) Murphy, G.; Nagle, P.; Murphy, B.; Hathaway, B. *J. Chem. Soc., Dalton Trans.* **1997**, 2645−2652.
(29) Maurya, M. R.; Agarwal, S.; Bader, C.; Rehder, D. *Eur. J. Inorg. Chem.* **2005**, 147−157.
(30) Cavaco, I.; Pessoa, J. C.; Duarte, M. T.; Matias, P. M.; Henriques, R. T. *Polyhedron* **1993**, *12*, 1231−1237.
(31) Manos, M. J.; Tasiopoulos, A. J.; Tolis, E. J.; Lalioti, N.; Woolins, J. D.; Slawin, A. M. Z.; Sigalas, M. P.; Kabanos, T. A. *Chem.−Eur. J.* **2003**, *9*, 695−703.
(32) Wulff-Molder, D.; Meisel, M. *Acta Crystallogr.* **2000**, *C56*, 33−34.
(33) Arrowsmith, S.; Dove, M. F. A.; Logan, N.; Antipin, M. Y. *J. Chem. Soc., Chem. Commun.* **1995**, 627−627.
(34) Salta, J.; Zubieta, J. *Inorg. Chim. Acta* **1996**, *252*, 435−438.
(35) Heinrich, D. D.; Folting, K.; Streib, W. E.; Huffman, J. C.; Christou, G. *J. Chem. Soc., Chem. Commun.* **1989**, 1411−1413.
(36) Karet, G. B.; Sun, Z.; Heinrich, D. D.; McCusker, J. K.; Folting, K.; Streib, W. E.; Huffman, J. C.; Hendrickson, D. N.; Christou, G. *Inorg. Chem.* **1996**, *35*, 6450−6460.
(37) Priebsch, W.; Rehder, D.; von Oeynhausen, M. *Chem. Ber.* **1991**, *124*, 761−764.
(38) Rieskamp, H.; Gietz, P.; Mattes, R. *Chem. Ber.* **1976**, *109*, 2090−2096.
(39) Crans, D. C.; Marshman, R. W.; Gottlieb, M. S.; Anderson, O. P.; Miller, M. M. *Inorg. Chem.* **1992**, *31*, 4939−4949.
(40) Carrano, C. J.; Mohan, M.; Holmes, S. M.; de la Rosa, R.; Butler, A.; Charnock, J. M.; Garner, C. D. *Inorg. Chem.* **1994**, *33*, 646−655.
(41) Herberhold, M.; Dietel, A. M.; Milius, W. *Z. Naturforsch. B: Chem. Sci.* **2003**, *58*, 299−304.

Table 5. Types of Tetranuclear Vanadium(V) Complexes with Organic Ligands[a]

type	core	coordination geometry	l(V−X)[b] (Å)	planarity (torsion angle of V_4)	conformation of V_4O_4 cycle	compound
A1	$\{V_4O_{16}\}$	SPY-5 $\{VO_5\}$ or OC-6 $\{VO_6\}$	2.19−2.32 (X = O)	P[c] (max ± 1°)	chair	$[V_4O_6(OCH_3)_6(acac)_2]\cdot 2CH_3CN$,[26] $[V_4O_6(OCH_3)_6(acac)_2]$,[26] $[V_4O_4\{(OCH_2)_3CCH_3\}_2(OCH_3)_6]$,[25] $[V_4O_4\{(OCH_2)_3CCH_3\}_3(OC_2H_5)_3]$[25]
	$\{V_4O_{12}N_4\}$	SPY-5, 2×$\{VO_3N_2\}$ 2×$\{VO_5\}$ or OC-6 2×$\{VO_4N_2\}$ 2×$\{VO_6\}$	2.27−2.33 (X = O)	P (max ± 1°)	chair	$[V_4O_8(OCH_3)_4(bpy)_2]$,[30] $[V_4O_8(OCH_3)_2(\mu_3\text{-}OCH_3)_2\text{-}(5,5'\text{-}Me_2bpy)_2]\cdot 3CH_3OH$[31]
A2	$\{V_4O_{16}\}$	SPY-5 $\{VO_5\}$ or OC-6 $\{VO_6\}$, $\{VO_5Cl\}$	2.56−2.89 (X = O, Cl, or nothing)	P (max ± 7°)	all μ-O above the V_4 plane	$(Ph_4P)[V_4O_8(CH_3COO)_4(NO_3)]$,[32] $(Ph_4As)[V_4O_8(CH_3COO)_4(NO_3)]$,[33] $(Ph_4P)[V_4O_8(CH_3COO)_4(Cl)]$,[34] $(NEt_4)_2[V_4O_8(NO_3)(tca)_4]\cdot H_2O$[d],35,36 $[V_4O_8(O_2CCH_2{}^tBu)_4]\cdot 2tBuCH_2COOH\cdot {}^tBuCH_2COOK$[37]
A3	$\{V_4O_{16}\}$	SPY-5 $\{VO_5\}$ or OC-6 $\{VO_6\}$	2.41, 2.46 (X = O)	P (max ± 7°)	two μ-O above the V_4 plane and two μ-O below the V_4 plane	$K_4[V_4O_8(C_2O_4)_4(H_2O)_2]\cdot 6H_2O$[38]
A4	$\{V_4O_{14}Cl_2\}$	SPY-5 $\{V_2O_7Cl\}$ or OC-6 $\{V_2O_9Cl\}$	2.271, 2.305 (X = O)	P		$[V_4O_4(OH)_2Cl_2(dmpd)_4]\cdot CHCl_3$[39]
A5	$\{V_4O_{16}\}$	SPY-5 $\{VO_5\}$ or OC-6 $\{VO_6\}$	2.487−2.749 (X = O)	NP	boat	this work
B1	$\{V_4O_8N_{12}\}$	OC-6 $\{VO_3N_3\}$	2.273, 2.268 (X = N)	NP	boat	$[V_4O_8\{BH(pz)_3\}_4]\cdot CH_2Cl_2\cdot 2H_2O$[40]
C1	$\{V_4O_8(C_5)_4\}$	quasi T-4 $\{VO_3C_5\}$		NP		$[V_4O_8(C_5H_5)_4]$[41]

[a] Abbreviations: acac = acetylacetonate(1−), Me_2bpy = 5,5′-dimethyl-2,2′-bipyridine, bpy = 2,2′-bipyridine, Ph_4P = tetraphenylphosphonium(1+), Ph_4As = tetraphenylarsonium(1+), tca = tiophene-2-carboxylato(1−), NEt_4 = tetraethylammonium(1+), $^tBuCH_2COOH$ = 3,3-dimethylbutanoic acid, dmpd = 2,2-dimethylpropane-1,3-diolate(2−), $BH(pz)_3$ = hydridotris(pyrazolyl)borate(1−). [b] X = atom in the trans position to the double-bonded O atom of the V═O_t group. [c] P = planar. NP = nonplanar. [d] The $[V_4O_8(NO_3)(tca)_4]^{2-}$ anion contains one delocalized electron. The average oxidation state of vanadium is 4.75 ($3 \times V^V + 1 \times V^{IV}$).

1.9328 Å for V−O_h; 2.0280−2.0542 Å for V−O_c. Each tartrato ligand possesses trans conformation with torsion angles 177.07° (for C1−C2−C3−C4) and 176.32° (for C5−C6−C7−C8) and forms two five-membered chelate rings. The tartrate anions are bonded as bis(bidentate) ligands, which is a common coordination mode for this anion.[23] The crystal structure of **1** is stabilized by numerous hydrogen bonds between water molecules and between water molecules and O atoms of the anions (O_t, O_b, and O_{tart}).

The structure of the chiral compound $(Et_4N)_4[V_4O_8((R,R)\text{-tart})_2]\cdot 6H_2O$ (**2**) consists of Et_4N^+ cations, $[V_4O_8((R,R)\text{-tart})_2]^{4-}$ anions, and molecules of water of crystallization. The structure of the $[V_4O_8((R,R)\text{-tart})_2]^{4-}$ ion is very similar to the structure of the anion in **1**. The coordination about the V atoms is a square-pyramid-like structure distorted toward a trigonal bipyramid ($\tau = 0.30$ for V1, $\tau = 0.12$ for V2, $\tau = 0.11$ for V3, and $\tau = 0.31$ for V4), and the arrangement of the $\{VO_5\}$ pyramids is analogous to the arrangement in the structure of **1**. Also, here weak interactions occur (l(V···O) values are 2.62 and 2.75 Å), which complete the coordination polyhedron of the central atoms to a strongly distorted octahedron.

The $[V_4O_8((R,R)\text{-tart})_2]^{4-}$ ions in the structure of **2** are connected by hydrogen bonds, and a two-dimensional (2D) layered structure is thus formed. Some of the Et_4N^+ cations are located in cavities that occur in the 2D sheets; the remainder are situated between the 2D layers.

A comparison of the structures of compounds **1** and **2** with those of other structurally characterized cyclic tetravanadates that have organic ligands bound to the V atoms and that contain exclusively or mostly vanadium(V) centers reveals some structural features (Table 5 and Figure 11). The 15 structures of this type from CCDC (July 2006) can be classified into several types.

Type A. The complexes of this type can be considered as constructed from the $\{VOE_4\}$ structural subunits possessing tetragonal-pyramidal geometry (SPY-5). The double-bonded O atom is always in the apical position; equatorial positions are taken by O or, exceptionally, N atoms. The $\{VOE_4\}$ subunits are often mutually arranged in a way that enables a weak covalent bonding (or weak interaction) between the V atom and a donor atom X (O or Cl) in the second apical position (trans position to the double-bonded O atom of the V═O_t group). The octahedral (pseudooctahedral) coordination geometry is thus achieved with V−X distances between 2.19 and 2.89 Å (Table 5). The structures classified into A1−A4 subtypes differ in the mode of arrangement of the $\{VOE_4\}$ subunits and in the positions of μ-O atoms relative to the V_4 plane (Figure 11).

Types B and C. With ligands that have special structural properties, the structures of type B ($[V_4O_8\{BH(pz)_3\}_4]\cdot CH_2Cl_2\cdot 2H_2O$) and type C ($[V_4O_8(C_5H_5)_4]$) are profoundly different from the structures of type A.

The structure of the $[V_4O_8(tart)_2]^{4-}$ ion presented here is unique, and although it is classified as type A5, it differs considerably from the other structures of type A. The four V atoms do not lie in one plane, and the $\{V_4O_4\}$ ring possesses a boat conformation. There is also another substantial difference between previously proposed structures of the $[V_4O_8(tart)_2]^{4-}$ ion[3,4,6] and the structure found by X-ray diffraction. In contrast to the arrangement in the proposed structure, the $tart^{4-}$ ligands do not bridge between adjacent V atoms of the $\{V_4O_4\}$ ring that are connected by μ-O atoms but instead coordinate to V1 and V2 or V3 and V4 (Figure

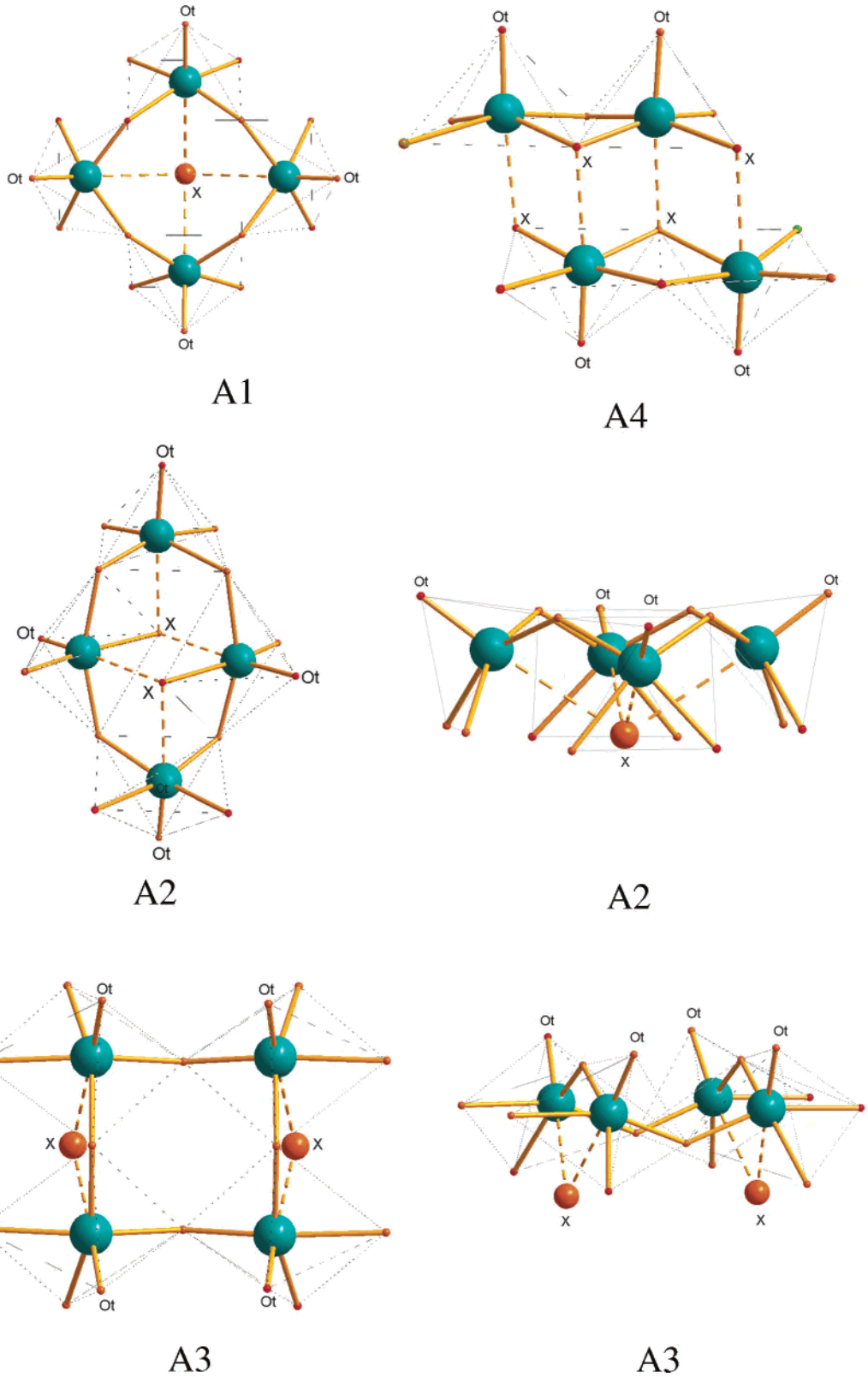

Figure 11. Types of tetranuclear vanadium(V) complexes with organic ligands (see text and Table 5). O_t = terminal oxygen atom; X = O or Cl atom trans to the O_t (or nothing in the case of $[V_4O_8(O_2CCH_2{}^tBu)_4]\cdot 2{}^tBuCH_2COOH\cdot {}^tBuCH_2COOK$[37]).

10). It is this unique binding mode that imposes the boat conformation on the $\{V_4O_4\}$ ring.

Acknowledgment. This investigation has been supported by the Ministry of Education of Slovak Republic (Grant VEGA 1/4462/07) and Comenius University in Bratislava (Grant UK/144/2006). NMR measurements were performed on the equipment supported by the Slovak State Programme Project No. 2003SP200280203. We thank Dr. Karel Doležal (Faculty of Natural Sciences, Palacký University, Olomouc, Czech Republic) for measurement of the ESIMS spectra.

Supporting Information Available: X-ray crystallographic files in CIF format for structures **1** and **2** and graphical representations of the formation of tartrate complexes (Figures 1s−5s). This material is available free of charge via the Internet at http://pubs.acs.org. Crystallographic data (excluding structure factors) for the structures have been deposited with the Cambridge Crystallographic Data Centre as supplementary publication nos. 622257 and 622258. Copies of the data can be obtained, free of charge, upon application to CCDC, 12 Union Road, Cambridge CB2 1EZ, U.K.

IC062223H